

Usefulness of three-dimensional digital subtraction angiography in endovascular treatment of a spinal dural arteriovenous fistula

Report of 2 cases

NORIAKI MATSUBARA, M.D., SHIGERU MIYACHI, M.D., TAKASHI IZUMI, M.D., TOMOTAKA OHSHIMA, M.D., ARIHITO TSURUMI, M.D., OSAMU HOSOSHIMA, M.D., TAKESHI KINKORI, M.D., AND JUN YOSHIDA, M.D.

Department of Neurosurgery, Graduate School of Medicine, Nagoya University, Nagoya, Japan

✓The use of 3D digital subtraction (DS) angiography provides a better understanding of spinal vascular lesion architecture. The authors report on 2 cases involving a spinal dural arteriovenous fistula (DAVF) and demonstrate the usefulness of 3D DS angiography for endovascular treatment of these spinal DAVFs. In both cases, middle-aged male patients suffered from bilateral leg hypesthesia, gait disturbance, and urinary dysfunction several months before treatment. Spinal angiography revealed DAVFs that were fed by a radicular artery branching from the intercostal artery and draining veins proceeding superiorly along the perimedullary veins. Endovascular embolization was performed in both cases. Selective 3D DS angiography of the intercostal artery clearly demonstrated the tortuous course of the feeder and the relationship among the feeding artery, fistula point, and draining veins in each case. This information was very useful in selecting a working angle for manipulating the microcatheter and for glue injection. In addition, the maximum intensity projection image from rotational DS angiography data clearly showed the fistula point at the dural sleeve and feeder entering the spinal canal via the intervertebral foramen and the relationship with the bone structure. Successful obliteration of the fistulae was achieved in both cases. Selective spinal 3D DS angiography was very useful in understanding the complex spinal vascular architecture and in choosing the best working angle and therapeutic strategy for endovascular treatment of spinal DAVFs. (DOI: 10.3171/SPI/2008/8/5/462)

KEY WORDS • endovascular embolization • spinal angiography • spinal dural arteriovenous fistula • 3D digital subtraction angiography

CURRENTLY, 3D rotational angiography has undergone widespread use. Rotational angiography is performed using the C-arm, which rotates around the patient's head in a few seconds. The rotational data are automatically transferred to a workstation, and this information allows us to obtain 3D DS angiography images a few minutes after rotational angiography. The 3D DS angiography images provide a better understanding of vessel architecture and vascular lesions. Many reports have underscored the usefulness of 3D DS angiography for intracranial vascular lesions, especially in the treatment of cerebral aneurysms;^{1–3,5–7,12} however, there have been few reports of the use of this methodology for other vascular disease-related

issues, including spinal vascular lesions. In this paper, we report 2 cases of spinal DAVFs and demonstrate the usefulness of 3D DS angiography for spinal vascular lesions.

Case Reports

Case 1

History and Examination. This 60-year-old male patient with a 1-year history of bilateral leg hypesthesia presented with gait disturbance and urinary hesitation 3 months before treatment. Spinal T2-weighted MR imaging showed an intramedullary high-intensity signal change and swelling on the spinal cord at T7–10 and a low-intensity signal on the dorsal side of the spinal cord indicating a flow void. Spinal angiography revealed a DAVF fed by the radicular artery branching from the left T-10 intercostal artery and a draining vein proceeding superiorly along the perimedullary veins. The artery of Adamkiewicz was detected by a

Abbreviations used in this paper: AVF = arteriovenous fistula; CT = computed tomography; DAVF = dural AVF; DS = digital subtraction; MIP = maximum intensity projection; MR = magnetic resonance; NBCA = *N*-butyl-cyanoacrylate.

Digital subtraction angiography for spinal DAVF

left T-9 intercostal artery angiogram and had no relationship with the DAVF.

Operation and Postoperative Course. We chose to perform endovascular embolization in this patient, because the DAVF was supplied by only a single feeding artery and a complete resolution was expected. The embolization was performed after local anesthesia was induced in the patient. A 4-Fr sheath was introduced from the right common femoral artery. The intercostal artery at T-10 underwent catheterization using a 4-Fr shepherd's hook-shaped catheter.

Rotational angiography was performed using the Axion Artis dBA system (Siemens AG). The rotational angle was $> 200^\circ$ and the rotational speed of the C-arm was $40^\circ/\text{second}$. Rotational data were acquired in a 960×960 matrix using a field-of-view 12-inch flat-panel detector. The data were then sent to the workstation (syngo X-Workplace, Siemens AG), which automatically produced a 3D DS angiography image, MIP image, and so on. The contrast material used in these cases was 300 mg/ml of non-ionic contrast medium. The rotational angiogram at T-10 was obtained using an injection delay of 0.5 seconds and an injection rate of 0.7 ml/second, for a contrast medium total volume of 4.1 ml.

Although the DAVF was difficult to understand in detail using conventional spinal angiography, selective 3D DS angiography at T-10 clearly demonstrated the tortuous course of the feeder and the relationship among the feeding artery, fistula point, and draining veins (Fig. 1A and B). In

addition, using the MIP images provided by rotational angiography data, we confirmed that the fistula point was located at the dural sleeve and confirmed its relationship with the surrounding architecture (the spinal canal, spinal cord, and vertebral body; Fig. 1C–E).

By manually rotating the 3D DS angiography image in a workstation, a precise working angle for manipulating a microcatheter and injecting glue was chosen based on this rotated image (Fig. 2A and B). Because the radicular artery branched off from the intercostal artery at a sharp angle in this case, the ventral branch was embolized using detachable coils in advance. The microcatheter was then manipulated to turn with the coil mass and guided into the target feeding artery (Fig. 2C). After provocative testing, 0.36 ml of 25% NBCA mixed with lipiodol was injected into the fistula using the microcatheter. This solution penetrated the drainage veins well, and successful obliteration of the fistula was achieved (Fig. 2D–G).

Postoperatively, the patient's paraparesis disappeared almost completely on the following day, and other symptoms such as urinary dysfunction and dysesthesia gradually improved. Although some high-intensity signal change of the spinal cord on T2-weighted MR imaging has remained, the abnormal flow void completely disappeared.

Case 2

History and Examination. This 50-year-old male patient initially presented with a 2-month history of bilateral leg

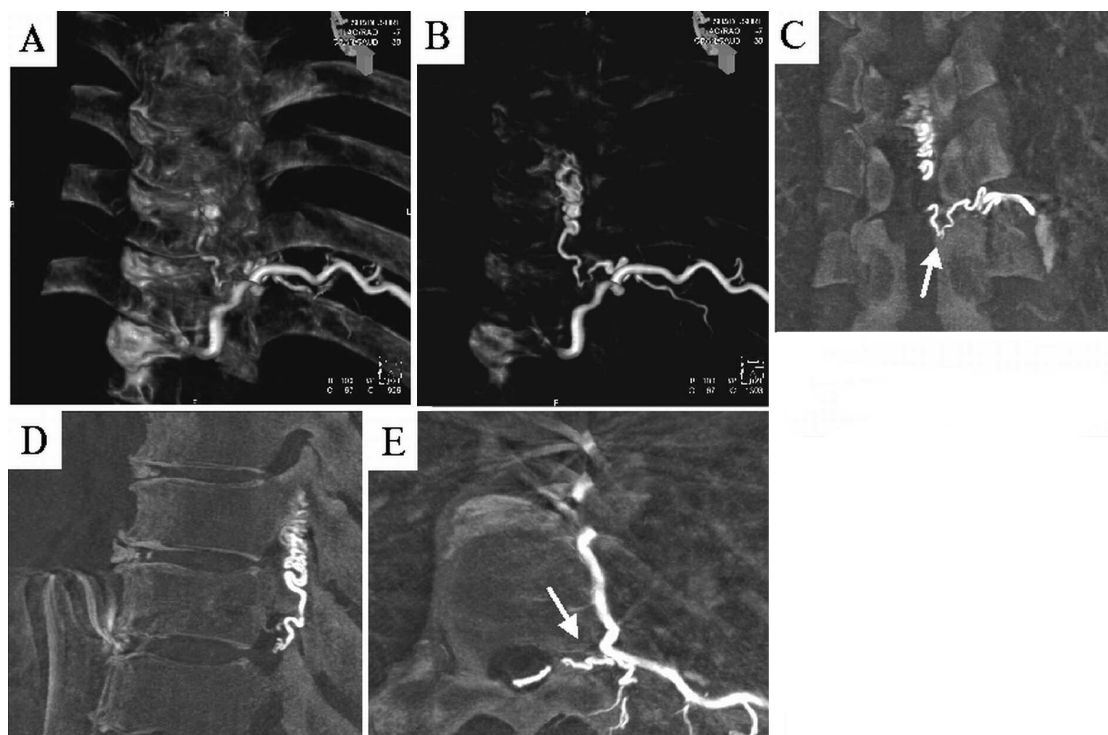


FIG. 1. Case 1. Three-dimensional DS angiography images (A and B) and MIP images (C–E) obtained from rotational angiography data showing the relationship between bone and vascular structures. The nonsubtraction (A) and subtraction (B) 3D DS angiography images demonstrate the tortuous course of the feeding artery and the relationship among the feeding artery, fistula point, and draining veins. In the 3 MIP images, the coronal image (C) shows the fistula point, which was clearly detected at the dural sleeve (arrow); the sagittal image (D) shows lesions on the dorsal side of the spinal cord; and the axial image (E) shows the feeding artery entering the spinal canal via the intervertebral foramen (arrow).

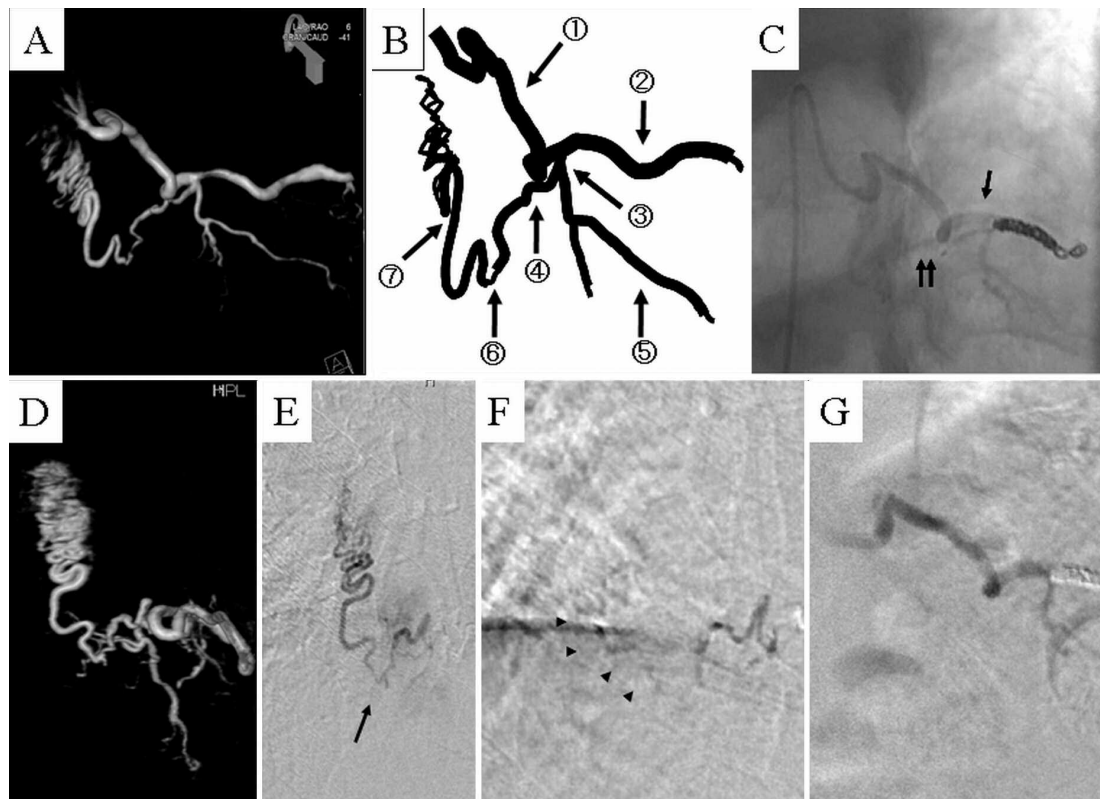


FIG. 2. Case 1. Images of the catheterization procedure. A: Selective T-10 3D DS angiography image of the working angle for catheterization clearly demonstrates the radicular artery sharply branching off from the intercostal artery. B: Schematic illustration of the vascular architecture in the patient showing the left T-10 intercostal artery (1), ventral branch (2), dorsal branch (3), radicular artery (4), posterior vertebral branch (5), fistula point (6), and draining vein (7). C: Left T-4 intercostal angiogram showing the microcatheter tip navigated into the radicular artery (double arrow) after coil embolization of the ventral branch (arrow). D: Selective T-10 3D DS angiography image of the working angle used for NBCA injection. E: Superselective angiogram, of a similar view as in panel D, from the working angle. The fistula point was clearly visualized (arrow). F: Angiogram showing injection of NBCA. The injection of NBCA penetrated into the draining vein (arrowheads). G: This T-10 angiogram obtained after embolization shows complete obliteration of the fistula.

hypesthesia and gait disturbance. Several days before treatment, however, his bilateral paraplegia and urinary dysfunction rapidly deteriorated.

Spinal T2-weighted MR imaging showed marked edema on the spinal cord at T1–L1 and flow void signal, which were similar to the results in Case 1. Spinal angiography revealed a DAVF fed by radicular arteries branching from the right T-6 (main feeder) and T-5 intercostal arteries. A very small artery of Adamkiewicz was detected on a right T-10 angiogram in this patient and had no relationship with the DAVF.

Operation and Postoperative Course. The deterioration of the patient's symptoms was so rapid that emergency endovascular embolization was performed. The intervention was performed after local anesthesia was administered to the patient. A 4-Fr sheath was introduced from the right common femoral artery and the T-6 intercostal artery first underwent catheterization using a 4-Fr cobra-shaped catheter.

Using the same angiography system as in Case 1, a rotational T-6 angiogram was obtained with an injection delay of 0.8 seconds at an injection rate of 1.0 ml/second,

for a contrast medium total volume of 6.0 ml. The precise working angle for catheterization and glue injection was determined using the manually rotated 3D DS angiography images from a workstation. A microcatheter was easily guided into the target feeding artery and the fistula was embolized with 0.4 ml of 25% NBCA (Figs. 3 and 4). Subsequently, the feeding artery from the T-5 intercostal artery was embolized using NBCA in the same manner, and total fistula obliteration was achieved. Postoperatively, the patient's symptoms, particularly paraplegia, were rapidly improved on the day following the operation.

Discussion

The understanding and classification of spinal cord vascular malformations and DAVFs have rapidly advanced with the development of sophisticated diagnostic equipment such as angiography and MR imaging apparatus.⁹ The main treatment method for these conditions has been direct operation, but the demand for using endovascular techniques has been increasing because it is a less invasive treatment option. For successful endovascular emboliza-

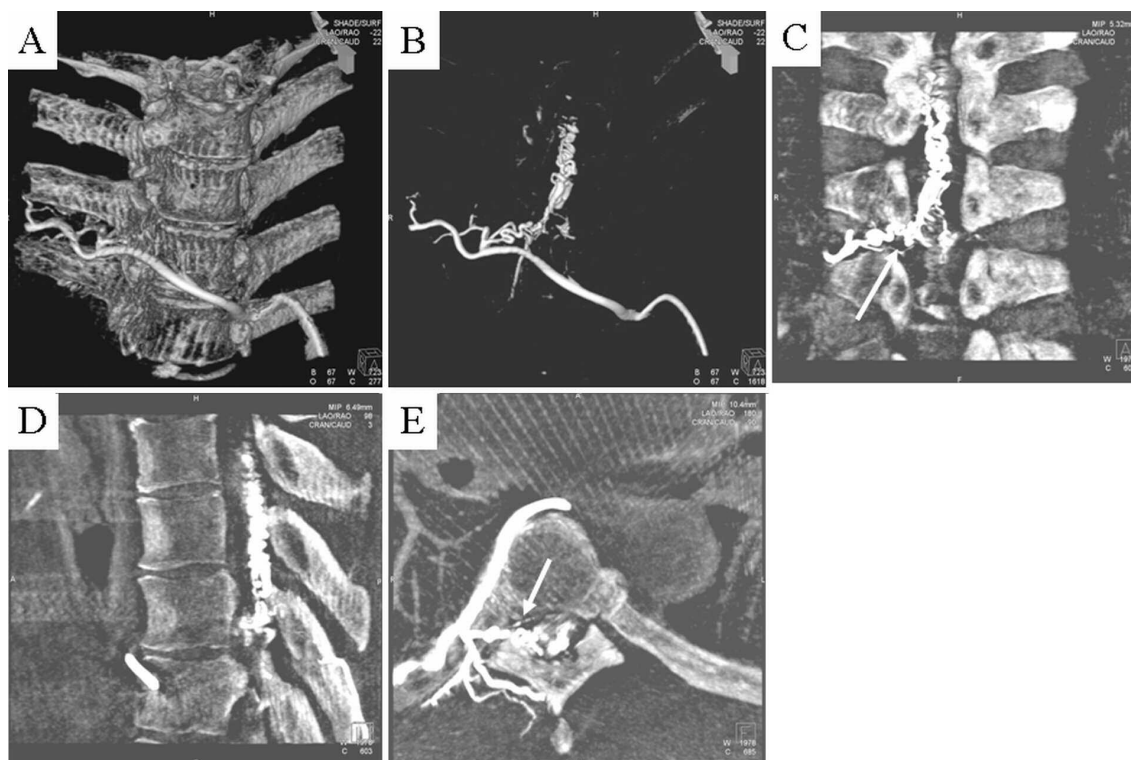


FIG. 3. Case 2. Three-dimensional DS angiography images (A and B) and MIP images (C–E) obtained from rotational angiography data. A and B: Selective nonsubtraction (A) and subtraction (B) T-6 3D DS angiography images show the relationship between bone and vascular structures similar to Case 1. C–E: Coronal (C), sagittal (D), and axial (E) MIP images of the DAVF obtained from the rotational DS angiography images. The fistula point is also clearly detected at the dural sleeve (*arrow*) as it was in Case 1.

tion, it is important that a microcatheter is selectively guided into the feeder branching off from the radicular artery as distally as possible, and a liquid material (such as NBCA) should be carefully injected to penetrate from the fistula point to the draining vein.^{13,17} For a spinal DAVF with a single or small number of feeders, as in these cases, there is a high possibility for a complete resolution using endovascular embolization alone.

Three-dimensional DS angiography clearly provides better comprehension of the 3D complex vessel architecture. Despite many reports of the usefulness of 3D DS angiography for intracranial vascular lesions, especially in connection with cerebral aneurysm embolization,^{1–3,5–7,12} only 3 studies provide an evaluation of this imaging procedure as applied to spinal vascular lesions.^{8,14,15}

Two case reports presented the usefulness of 3D DS angiography in the treatment of spinal hemangioblastoma.^{8,15} Kern and colleagues⁸ indicated the usefulness of spinal 3D DS angiography for preoperative examination and surgical planning for a thoracic spinal nerve hemangioblastoma. Sciubba and associates¹⁵ also reported the use of 3D DS angiography in 2 cases of cervical spinal cord hemangioblastoma. Prestigiacomo et al.¹⁴ disclosed 17 selective spinal 3D DS angiograms acquired in 14 cases of spinal arteriovenous malformation, AVF and DAVF. These investigators concluded that selective spinal 3D DS angiography is an excellent adjunct to conventional DS angiography, providing clinicians better information about the relation-

ships among the feeding arteries, nidus, aneurysm, draining vein, and bone structure; helping to discriminate between intramedullary or perimedullary lesions; and for selecting the precise working angle for catheterization and treatment, and therefore assisting in treatment strategy decisions. In addition, use of 3D DS angiography reduces the total radiation dose that is necessary.¹⁴

In our 2 cases, the relationships between the DAVF and the bone structure were confirmed by using 3D reconstruction images (subtraction and nonsubtraction) and MIP images together. This information served to pinpoint the fistula location on the dural sleeve, as well as the feeders entering the spinal canal via the intervertebral foramen and draining veins running along the dorsal side of the spinal cord. In addition, manually rotated 3D DS angiography images on the workstation were very helpful in selecting the best working angle from which to sufficiently identify a feeder of the radicular artery branching off from the intercostal artery, fistula point, and draining vein.

Depiction of the 3D structure of the spinal vascular lesion and fistula identification may be possible in 3D CT angiography,^{10,18,19} and is especially useful when the bone structure is involved. The image resolution of 3D CT angiography, however, is inferior to that provided by selective 3D DS angiography, because contrast medium is not injected selectively into an intercostal artery. Also, improper timing from the injection of contrast medium until filming may result in mixing of the arterial and venous phases

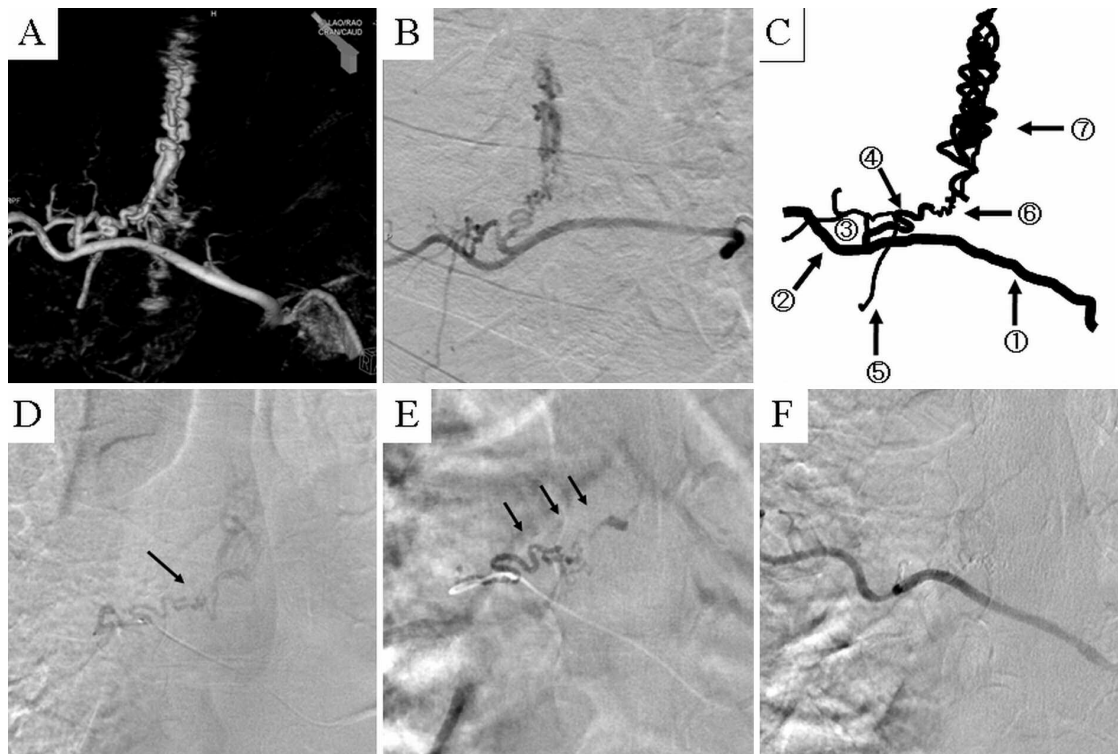


FIG. 4. Case 2. Images of the catheterization procedure. A: A selective T-6 3D DS angiography image of the working angle used for catheterization and NBCA injection. B: Selective T-6 angiogram of a similar view to panel A. C: Schematic illustration of the vascular architecture in the patient showing the left T-6 intercostal artery (1), ventral branch (2), dorsal branch (3), radicular artery (4), posterior vertebral branch (5), fistula point (6), and draining vein (7). D: Angiogram of the feeding artery from the working angle. The fistula point is clearly visualized (*arrow*). E: Angiogram showing the injection of NBCA, which penetrated into the draining vein (*arrows*). F: This T-6 angiogram after embolization shows no filling of the fistula.

and thus result in a poor image. A problem can also occur when subtracting the surrounding structure and reconstructing the 3D CT angiography image if some type of artifact reaches an adjacent vascular structure in a narrow spinal canal.

Magnetic resonance angiography has also become an option for these lesions. The latest MR imaging technology may depict spinal cord vascular lesions in 3D using contrast medium or 3D image-processing software.^{4,11,16,19} Use of MR angiography has a disadvantage, however, because it cannot provide a sufficiently precise image to determine the relationship of the lesion with surrounding bone structure. An additional drawback of using MR angiography is that an artifact due to body movement and thoracic motion synchronized with breathing can easily adversely affect the image. Thus, the imaging resolution provided by spinal MR angiography is generally not sufficient for endovascular treatment.

Conventional spinal angiography is essential for evaluation of spinal vascular disease, but it is also adversely affected by motion artifacts due to heartbeat, breathing, or bowel peristalsis. General anesthesia and administration of glucagons are available to correct these problems, but there are limitations to the use of these corrections. Conventional angiography provides only 2D imaging, but selective 3D DS angiography provides optimal 3D vascular images. A flat-panel detector can obtain more exact data with rota-

tional selective spinal angiography and high-speed C-arm rotation. Additionally, high-performance image revision software can make artifacts produced by minute body movements disappear in the process of 3D reconstruction and can thus provide clear 3D DS angiography images.

If angiography timing is adequately set, 3D DS angiography can clarify only the shunt point in the case of an arteriovenous fistula. Furthermore, because the workstation provides a direct link with the angiography system apparatus, the 3D DS angiography image can be used as a reference immediately, depending on the therapeutic method and strategy used.

Use of 3D DS angiography does have limitations. For example, in selective 3D DS angiography, image defects may occur in cases of a high-flow spinal arteriovenous malformation, because the rotation speed of the C-arm cannot catch up to the shunt flow. Less visibility of tiny vessels, lack of visibility of part of the venous structure, and temporal resolution of blood flow are also drawbacks to using 3D DS angiography, but technical improvements are expected in the near future.

Conclusions

We report on 2 patients with spinal DAVFs whose vascular structures were clearly visualized using selective spinal 3D DS angiography. This 3D DS angiography approach

proved very useful for understanding the complex spinal vascular architecture, selecting the best working angle, and developing an appropriate therapeutic strategy during endovascular treatment for these spinal DAVFs. The usefulness of this procedure assures good operative and clinical outcomes for patients with these lesions.

References

1. Abe T, Hirohata M, Tanaka N, Uchiyama Y, Kojima K, Fujimoto K, et al: Clinical benefits of rotational 3D angiography in endovascular treatment of ruptured cerebral aneurysm. **AJNR Am J Neuroradiol** **23**:686–688, 2002
2. Anxionnat R, Bracard S, Ducrocq X, Troussset Y, Launay L, Kerrien E, et al: Intracranial aneurysms: clinical value of 3D digital subtraction angiography in the therapeutic decision and endovascular treatment. **Radiology** **218**:799–808, 2001
3. Anxionnat R, Bracard S, Macho J, Da Costa E, Vaillant R, Launay L, et al: 3D angiography. Clinical interest. First applications in interventional neuroradiology. **J Neuroradiol** **25**:251–262, 1998
4. Binkert CA, Kollias SS, Valavanis A: Spinal cord vascular disease: characterization with fast three-dimensional contrast-enhanced MR angiography. **AJNR Am J Neuroradiol** **20**:1785–1793, 1999
5. Gailloud P, Oishi S, Carpenter J, Murphy KJ: Three-dimensional digital angiography: new tool for simultaneous three-dimensional rendering of vascular and osseous information during rotational angiography. **AJNR Am J Neuroradiol** **25**:571–573, 2004
6. Gauvrit JY, Leclerc X, Vermandel M, Lubicz B, Despretz D, Lejeune JP, et al: 3D rotational angiography: use of propeller rotation for evaluation of intracranial aneurysm. **AJNR Am J Neuroradiol** **26**:163–165, 2005
7. Hochmuth A, Spetzger U, Schumacher M: Comparison of three-dimensional rotational angiography with digital subtraction angiography in the assessment of ruptured cerebral aneurysms. **AJNR Am J Neuroradiol** **23**:1199–1205, 2002
8. Kern M, Nacini R, Lehmann TN, Benndorf G: Imaging of thoracic spinal nerve haemangioblastoma by three-dimensional digital angiography. **J Clin Neurosci** **13**:929–932, 2006
9. Kim LJ, Spetzler RF: Classification and surgical management of spinal arteriovenous lesions: arteriovenous fistula and arteriovenous malformation. **Neurosurgery** **59** (5 Suppl):S195–S201, 2006
10. Lai PH, Pan HB, Yang CF, Yeh LR, Hsu SS, Lee KW, et al: Multi-detector row computed tomography angiography in diagnosing spinal dural arteriovenous fistula: initial experience. **Stroke** **36**:1562–1564, 2005
11. Mascalchi M, Cosottini M, Ferrito G, Quilici N, Bartolozzi C, Villari N: Contrast-enhanced time-resolved MR angiography of spinal vascular malformation. **J Comput Assist Tomogr** **23**:341–345, 1999
12. Missler U, Hundt C, Wiesmann M, Mayer T, Brückmann H: Three-dimensional reconstructed rotational digital subtraction angiography in planning treatment of intracranial aneurysms. **Eur Radiol** **10**:564–568, 2000
13. Niimi Y, Berenstein A, Setton A, Neophytides A: Embolization of spinal dural arteriovenous fistulae: results and follow-up. **Neurosurgery** **40**:675–683, 1997
14. Prestigiacomo CJ, Niimi Y, Setton A, Berenstein A: Three-dimensional rotational spinal angiography in the evaluation and treatment of vascular malformations. **AJNR Am J Neuroradiol** **24**:1429–1435, 2003
15. Sciubba DM, Mavinkurve GG, Gailloud P, Garonzik IM, Recinos PF, McGirt MJ, et al: Preoperative imaging of cervical spine hemangioblastomas using three-dimensional fusion digital subtraction angiography. Report of two cases. **J Neurosurg Spine** **5**:96–100, 2006
16. Shigematsu Y, Korogi Y, Yoshizumi K, Kitajima M, Sugahara T, Liang L, et al: Three cases of spinal dural AVF: evaluation with first-pass, gadolinium-enhanced, three-dimensional MR angiography. **J Magn Reson Imaging** **12**:949–952, 2000
17. Song JK, Gobin YP, Duckwiler GR, Murayama Y, Frazee JG, Martin NA, et al: N-butyl 2-cyanoacrylate embolization of spinal dural arteriovenous fistulae. **AJNR Am J Neuroradiol** **22**:40–47, 2001
18. Yamaguchi S, Eguchi K, Kiura Y, Takeda M, Nagayama T, Uchiida H, et al: Multi-detector-row CT angiography as a preoperative evaluation for spinal arteriovenous fistulae. **Neurosurg Rev** **30**:321–327, 2007
19. Zampakis P, Santosh C, Taylor W, Teasdale E: The role of non-invasive computed tomography in patients with suspected dural fistulas with spinal drainage. **Neurosurgery** **58**:686–694, 2006

Manuscript submitted November 26, 2007.

Accepted January 10, 2008.

Address correspondence to: Noriaki Matsubara, M.D., 65 Tsurumai-cho, Showa-ku, Nagoya, Aichi 466-8550, Japan. email: mnoriaki0817@yahoo.co.jp.